

# Spring-block approach for crack patterns in glass

Research Article

Emőke-Ágnes Horvát<sup>1\*</sup>, Ferenc Járαι-Szabó<sup>2†</sup>, Yves Brechet<sup>3‡</sup>, Zoltán Nédա<sup>2§</sup>

1 Interdisciplinary Center for Scientific Computing, University of Heidelberg, Speyererstr 6, 69115 Heidelberg, Germany

2 Department of Theoretical and Computational Physics, Babeş-Bolyai University,  
Str. Kogălniceanu 1, RO-400080, Cluj-Napoca, Romania

3 Grenoble Institute of Technology, ENSIMAG, Grenoble, France

**Abstract:** Fracture patterns resulting from point-like impact acting perpendicularly on the plane of a commercial soda-lime glass plate is modeled by a spring-block system. The characteristic patterns consist of crack lines that are spreading radially from the impact point and concentric arcs intersecting these radial lines. Experimental results suggest that the number of radial crack lines is scaling linearly with the energy dissipated during the crack formation process. The elaborated spring-block model reproduces with success the observed fracture patterns and scaling law.

**Keywords:** brittle fracture • pattern selection • spring-block models

© Versita Warsaw and Springer-Verlag Berlin Heidelberg.

## 1. Introduction

Glass is one of the oldest and most commonly used materials in our everyday life and engineering [1]. For different practical applications diverse geometrical forms are needed, but the most widespread shapes are in the form of thin plates. Unfortunately for many engineering applications soda-lime glass plates are quite brittle materials, rather sensitive to shocks acting perpendicularly on them [2]. In laymen terms this means they can easily break. When a projectile with enough momentum hits a glass-plate, characteristic fracture patterns are generated (see Fig.1). The crack structure which is observed under such loading consist of a few concentric circles or arcs and many radial crack lines initiating from the impact point. The number of radially spreading crack lines depends on the strength of the impact, and the number of concentric circle shaped cracks depends both on the loading, thickness of the glass plate and fixing conditions for the plate. By varying these parameters the cracks patterns can slightly change, although the two characteristic crack-types (circle and radial) are clearly visible. In Figure 2

\* *E-mail:* agnes.horvat@iwr.uni-heidelberg.de

† *E-mail:* jferenc@phys.ubbcluj.ro

‡ *E-mail:* yves.brechet@simap.grenoble-inp.fr

§ *E-mail:* zneda@phys.ubbcluj.ro

we present a small collection of crack patterns obtained by a point-like impact. Understanding such fracture or fragmentation patterns and modeling them is a challenge for modern computational material science and physics [3–9].

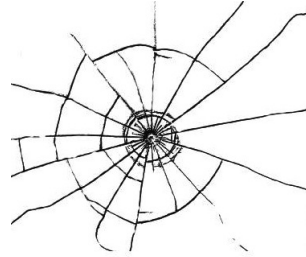


**Figure 1.** Characteristic fracture pattern on a glass plate produced by a localized perpendicular shock. The radial and arc-like crack lines are nicely observable.

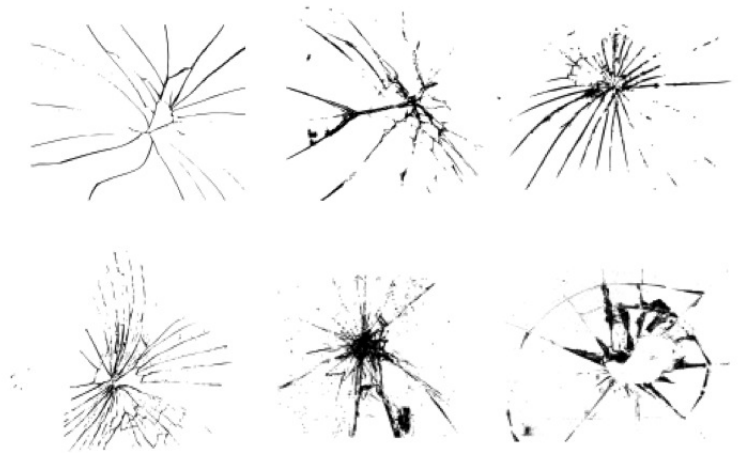


**Figure 2.** A collection of crack patterns induced by a localized perpendicular impact on glass plates.

Fracture and elasticity of soda-lime glass has been studied and modeled for a long time [10–16]. Recently it has been experimentally proven that fracture in glass is brittle [17]. Engineering aspects (for a recent review see [18, 19]) were studied by indentation experiments quite early, starting with the pioneering work of Auerbach [20]. Many simple and less sophisticated kitchen-type experiments were made by statistical physicists aiming to understand the pattern formation phenomenon and collective behavior of crack-lines for various type of uniformly distributed loading [21–23]. Simple models and theoretical arguments were considered already in the early 90’s for describing the obtained structures [24–27]. The present paper intends also to contribute in such sense. Our

aim here is to show, that a simple spring-block type model for fracture and fragmentation is appropriate for qualitatively describing the observed patterns and can also successfully reproduce some quantitative scaling laws revealed in experiments.

## 2. Spring-block models

A simple mechanical system of blocks interconnected under various topologies by springs and sliding on a frictional surface proved to be helpful for approaching many complex phenomena. As a first application of this system, one should mention Burrige and Knopoff [28], who first used a dragged spring-block-chain to successfully explain the Guttenberg-Richter [29] scaling-law for the earthquake magnitudes. As a recognition of their results, nowadays spring-block models are also labeled as Burrige-Knopoff type models. The model was generalized in two dimension by Olami, Feder and Christensen [30]. Afterwards, due to the spectacular evolution of computers and computer simulation methods, the spring-block model proved to be useful in describing other phenomena as well. The model is especially appropriate for those problems where avalanche-like dynamics or pattern formation is present. Known examples in this respect are the Portevin-Le Chatelier phenomena [31], the Barkhausen noise [32], formation of traffic jams [33], structures formed by the capillary self-organization of nano-particle systems [34, 35] or fragmentation and fracture of various materials under different loading [36].

The fascinating polygonal patterns obtained in dried mud are familiar to everyone. Such patterns hide also an interesting scaling law, which connects the average fragment area with the layer thickness. One success of the spring-block-type models was the elegant reproduction of these patterns and scaling law. In this approach the grains of the material are modeled by blocks sliding on a two-dimensional substrate, while the capillarity effect of drying water which leads to fragmentation is modeled by springs interconnecting the blocks [37, 38]. Initially, the blocks are placed on the sites of an abstract triangular lattice and first neighbors are interconnected by springs. A small amount of stochasticity is introduced by displacing randomly the blocks relative to their original position on the lattice. The springs are then stressed and a relaxation dynamics is imposed on the system. During this dynamics: (i) each block will slide to a new equilibrium position when the total force acting on it is greater than the friction force and (ii) each spring is allowed to break whenever the tension in it exceeds a breaking threshold. Several layers of springs are considered in order to incorporate the thickness of the material in the model. Due to the competing effects of the spring tensions and frictional forces, blocks will slide in avalanches leading finally to the breakage of the springs and thus to fragmentation of the system. Very realistic fracture lines and fragmentation topologies are obtained. By using this simple spring-block model one could get precious information about the role of the main controllable physical parameters in the final crack pattern. A similar spring-block type model was used for explaining the formation of fascinating spiral shaped fracture structures in drying precipitates [39, 40]. To reproduce these continuously bending crack lines an additional stress front moving towards the centre of the two-dimensional system was used. This stress front modeled the advancing drying front

in the fragment, which was believed to be responsible for the formation of the spiral shaped cracks. Motivated by the successes of the spring-block type models in describing fracture and fragmentation, we adapt this model for describing crack patterns in glass plates subjected to localized shocks acting perpendicularly to the plate.

### 3. A model for glass fracture

We will consider a two-dimensional spring-block approach for describing fracture patterns in glass. A first attempt to use such model for brittle fracture was made by Curtin and Scher in the early 1989 [41]. A natural question that one can immediately raise is how can crack generation and propagation, which are typically plastic behaviors, be approached with springs, that are perfectly elastic elements. The answer to this is that beside the elastic spring forces we consider energy dissipating friction forces and spring breaking events. Our first aim is to make realistic the spring-block model for glass-like systems by incorporating the following features of glasses: the amorphous structure, the elastic response to small stresses by a local reorganization and the plasticity in case of high stresses. In order to match these requirements within the framework of the spring-block models some changes have to be done relative to the model originally used by us for fracture and fragmentation of granular materials.

The elaborated model is two-dimensional and its main elements are blocks which can move hindered by friction and springs connecting them. Disk shaped blocks, all with the same radius  $r_0$  will model mesoscopic elements of the glass while the cohesion forces between them are modeled by elastic springs. These springs have all of them the same spring constant  $k$ , and their length is defined as the distance between the centers of the connected blocks. The spring tension is  $F_k = k \cdot r$  for lengths  $r$  between  $2r_0 \leq r \leq r_{max}$ , where  $r_{max}$  is the breaking threshold (maximal allowed elongation) of the springs. In the spring force it is also included a hard-core type repulsion which forbids blocks to interpenetrate each other. This repulsion is described by the repulsive part of a Lenard-Jones-type potential. The force-profile of the forces acting in the springs is sketched in Figure 3a.

The friction forces acting on the blocks models the pinning forces that are opposing the unrestricted rearrangement of the mesoscopic elements in a glass sample subjected to stress. Within our spring-block approach the friction acts between the blocks and the surface. It can equilibrate a net force less than  $F_{fmax}$ . Whenever the total force  $F_i(i)$  acting on a block  $i$  exceeds this  $F_{fmax}$  value the block begins to slip with an over-damped motion. This force profile is borrowed from classical mechanics, where we assumed that the static friction force is able to equilibrate a net force which is less than the static friction force value. Similar approach has been used with success to model pinning forces acting on nano-scale objects [34]. The characteristic profile of the friction forces is illustrated in Figure 3b. In order to incorporate in the model the quasi-disordered nature of glass at mesoscopic level the  $F_{fmax}$  slipping threshold values are randomly distributed on the surface. For implementing this quenched disorder, we consider a cellular division of the surface. For the sake of simplicity we construct uniform cells using a square lattice topology (Figure 4). In each cell a randomly chosen  $F_{fmax}$  threshold force is assigned. In order to achieve this, we generate uniformly distributed random numbers between two fixed limits:  $F_{f1}$  and  $F_{f2}$ . The lattice

constant of this auxiliary cellular structure is chosen to be of the same order of magnitude as the value of  $r_0$ .

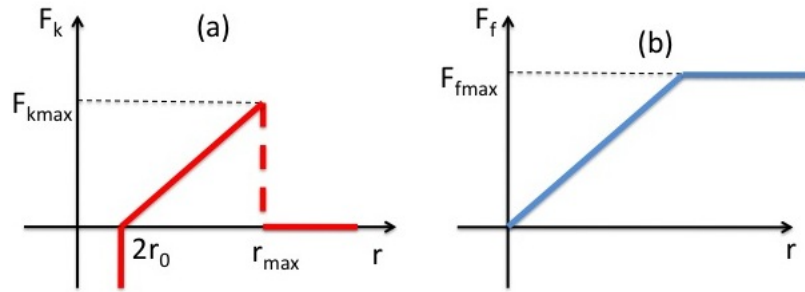


**Figure 3.** Force profiles for the spring forces (a) and friction forces (b).

The blocks are initially placed on the sites of a triangular lattice. To introduce an isotropy in this symmetric structure we randomize the initial distribution by displacing the blocks randomly from their original site, and relaxing the system so that the blocks should not overlap. By this step, a secondary disorder and an isotropy characteristic for amorphous systems is introduced. Due to the random friction values this equilibrium state will have internal stresses frozen into the system. We connect now neighboring blocks by considering springs between those blocks, for which the centers can be connected without intersecting another block and the distance is smaller than  $r_{max}$  (these conditions will be referred later as the *geometric condition*). In this way, an initially pre-stressed and isotropic spring-block network is built.

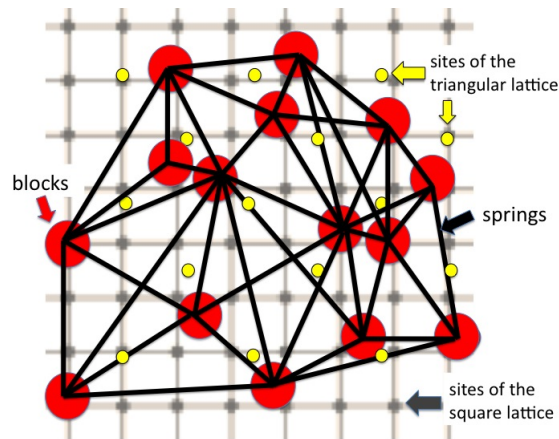


**Figure 4.** Construction of the initial isotropically interconnected spring-block network.

The simulation has two main parts.

In the first part of the simulation the initially constructed and pre-stressed spring-block system is relaxed to an equilibrium configuration where all spring-tensions are less than the breaking threshold (springs with higher tension are broken), the resulting forces acting on blocks are less than the friction thresholds and the blocks do

not overlap.

In the second part of the simulation the external shock is applied and the system is relaxed again. The impact is applied by increasing the spring constants in the system following a reasonable stress profile. Our intention is to model the fracture of glass-plates due to a point-like perpendicular shocks. A simple exponentially decaying stress profile was chosen in the form of  $k_{extra} = k_0 \cdot \exp(-r/\lambda)$ , where  $r$  is the distance from the impact point,  $\lambda$  is a characteristic decay distance and  $k_0$  is the magnitude of the point-like perturbation. After this additional loading is applied the system is relaxed again. During this relaxation process cracks are nucleating and propagating in the system. The time evolution of the systems is recorded and from this data the crack evolution process and the final crack structure is investigated.

For both parts of the simulation the relaxation process is realized in a similar manner, following the same relaxation steps. Instead of a time-consuming rigorous classical molecular dynamics simulation we have chosen to follow a simpler method based on the assumption of an overdamped dynamics of the blocks. The same approach was used previously in simulating the fragmentation of drying nano-sphere system [34]. Due to the fact that we are not interested here in the real time-like dynamics, the time length  $dt$  for each relaxation step is taken as unity ( $dt = 1$ ) and the following moves are done:

1. *Reorganization.* At the beginning of each relaxation step the spring system is reconstructed by respecting *the geometric condition*. By this the isotropy of the system is restored and the elasticity of glass is approximated.
2. *Recalculation of forces.* The resultant force acting on each block  $i$  is computed as:  $\vec{F}_t(i) = \sum_p d_{ip} \vec{F}_k(i, p)$ , where the sum is over all the other blocks  $p$ , and  $d_{ip}$  is 1 if the blocks are connected by spring and 0 otherwise, and  $\vec{F}_k(i, p)$  is the tension in springs connecting blocks  $i$  and  $p$ .
3. *Slipping of the blocks.* The total force  $\vec{F}_t(i)$  acting on each block  $i$  is analyzed. If its magnitude  $F_t(i) = |\vec{F}_t(i)|$  is bigger than the  $F_{fmax}$  threshold, the block will slip with an over-damped motion. Over-damped motion appears when the resistance forces acting on behalf of a continuous medium on a moving body are increasing sharply with its velocity. Often in such cases a limit velocity is very quickly reached. This limit velocity depends on the applied force and it is governed by a viscous damping coefficient  $\eta$ . The reciprocal value of this damping coefficient is called *mobility*. During an over-damped motion we assume no acceleration, and consider the velocity proportional with the acting force and mobility. In a time interval  $dt$  the position of the block will change by:  $d\vec{r}_i = \vec{F}_t(i)dt/\eta$ . The repulsive interaction incorporated in the spring forces forbids the blocks to slide on each other and the presence of viscous damping eliminates unrealistic oscillations.

The relaxation step consisting of the above presented consecutive moves is repeated until a step is finished without having any disk slipping event. Since a perfect relaxation is hard to achieve, a very small tolerance level is considered and it is assumed that the relaxation is completed when the maximal slip in the system is smaller than this tolerance value.

Before starting however the simulations first the geometry of the simulated plates has to be fixed. Due to the rotational symmetric shock profile, we present the final results on a disk-like plate. Nevertheless, for the sake of computational simplicity and for minimizing edge effects simulations are done on a much larger square-like domain.

Another crucial point of simulations is to define boundary conditions for the relaxing system. In principle several types of boundary conditions might be possible to impose, but we will see that the majority of them will have shortcomings. The problem of boundary conditions in such systems were analyzed in detail in a previous work considering the capillary self-organization of nanospheres [34].

A natural solution would be to use free boundary condition which can be realized in a simple manner by positioning initially the blocks inside the simulated area. After connecting the blocks by springs as described earlier, the blocks on the edges and corners will experience a resultant net force in the direction of the center. In the first part of the simulation the system would compact unevenly due to this unbalanced net force and therefore a non-homogeneously pre-stressed system would form. Using thus free boundary conditions is not advisable.

To eliminate the initial non-homogeneous contraction of the system one can consider periodic boundary conditions. Periodic boundary conditions are however not useful here since it would lead to unrealistic crack lines that are leaving the system in one side and entering on the other side and thus self-interacting.

The best solution is to use fixed boundary conditions. This can be realized by positioning again the blocks inside a square and considering a chain of fixed blocks on the chosen perimeter. These fixed blocks are connected between their neighbors with geometrically allowed springs. The system is stabilized, and the initial construction of the isotropically pre-stressed spring-block network is done. The fixed boundary conditions will have influence on the crack propagation dynamics only in the later stages where the cracks are reaching the edges, decreasing the propagation speed of the radially oriented crack lines. In order to diminish the influence of this unrealistic effect over the morphology of the final crack configurations, as we have already stated previously, we will present results only for an inner disk shaped part of the simulated system.

## 4. Model parameters

At a first glance one might get concerned that the spring-block model presented in the previous section has too many freely adjustable parameters. We will see however that most of the parameters can be fixed by simple arguments and only a few main controllable parameters are of importance for us.

Let us discuss now the model parameters.

- The unit length in the system is defined by the *size of the disks*. So it has been considered  $r_0 = 1$ .
- *Size of the simulated system*. Evidently the best would be to have as large system as possible in order to minimize the effect of edges. Our computational resources allowed us to study systems of sizes up to  $600 \times 600$  blocks and the used disk shaped region had usually a radius of  $200r_0$ , containing around 125000

blocks.

- One of the parameters that will appear immediately at the initiation stage is the level of *space filling for the blocks* related to  $r_0$  and the lattice constant of the used triangular lattice. This space-filling parameter can be defined as  $\rho = S/(N\pi r_0^2)$ , where  $S$  is the simulation area and  $N$  is the number of blocks in the system. Since we are simulating a continuous media, one has to deal with high, almost close-packing space filling. In order to allow also for slipping we have chosen a convenient  $\rho = 0.85$  value for most of our simulations.
- The force units are defined through the value of *the spring-breaking threshold*. Accordingly,  $F_{kmax} = 1$  was imposed.
- An important parameter is the initial value of *the spring constants,  $k$* . It is desirable to choose the value of  $k$  so that only a small fraction of springs should break initially, such that our model system is as compact as possible. Combining with the other choices of the force-like parameters we have found that a value of 0.4 units yields a good initial structure with enough frozen stresses and few bonds that are broken.
- The parameter which governs *the repulsive part of the spring force*. This can be chosen quite arbitrarily, the only condition we have to respect is to have no repulsion at the distance  $2r_0$  and a strong hard-core type repulsion for smaller distances. We have chosen this force as the repulsive part of the Lenard-Jones potential  $F_r(2r_0 - r) = \sigma(2r_0 - r)^{12}$  with  $\sigma = 10$ , chosen arbitrarily. Other values for  $\sigma$  would not alter significantly our results.
- *The viscous damping coefficient  $\eta$* . The model will only work for values chosen between reasonable limits, and for these viscous damping values the final patterns are rather similar. Choosing a too small value will result in unrealistic oscillations of the blocks, while a too high value will make the block slip too small and increase considerably the relaxation time. In the present simulations we have chosen the  $\eta = 100$  value.
- *The parameters of the applied stress*. As discussed already the applied loading has a rotationally symmetric and exponentially decaying form:  $k_{extra} = k_0 \cdot \exp(-x/\lambda)$ . The characteristic decay distance was chosen as  $\lambda = 30$  and the  $k_0$  parameter was the main parameter governing the strength of the applied shock.
- The interval  $[F_{f1}, F_{f2}]$  from where *the pinning force values* are randomly drawn. This is the second free parameter set of the model, allowing to study the effect of disorder in the system.
- *The lattice constant* of the underlying square lattice on which the disorder in the friction forces is realized. Together with the  $F_{f1}$  and  $F_{f2}$  parameters this can also influence the disorder level in the system. Since we have chosen to control the disorder level with  $F_{f1}$  and  $F_{f2}$ , we have fixed this lattice constant to the  $r_0$  value.

As detailed above only a few parameters of the model are not fixed by simple conceptual considerations. We remain thus with the following parameters that will govern the generated patterns: the magnitude of the external

shock loading and the  $F_{f1}$  and  $F_{f2}$  values governing the disorder in the studied material. The influence of these parameters on the final crack structure was investigated by large-scale computer simulations.

## 5. Simulation results

Large-scale computer simulations were performed to analyze the influence of the applied shock intensity and disorder in the friction forces. To complete one simulation on a large  $S = 600 \times 600$  system several weeks of computing were necessary on the computer cluster available for us. By using the parameter set specified in the previous section the reproduction of the radially spreading crack-lines was quite straightforward (Figures 5 and 6). The obtained time evolution of cracks and the final crack patterns are quite realistic. A typical time-evolution sequence is shown in Figure 5 for two applied shock intensities. In agreement with our expectations we got that with increasing shock intensity (governed by the  $k_0$  parameter) the number of radially spreading crack lines are also increasing. Besides the radially oriented crack lines a circle shape crack-line is also observable at a distance of the order of  $\lambda$ . The radius of this concentric crack line is increasing with the intensity of the applied shock. One can also observe that the obtained patterns have an increased rotational symmetry relatively to those presented in Figures 1 and 2. The explanation of this is simple: in our computer simulation experiments we have always used a completely rotationally symmetric stress profile, while in real-life experimental situations rarely is this the case.

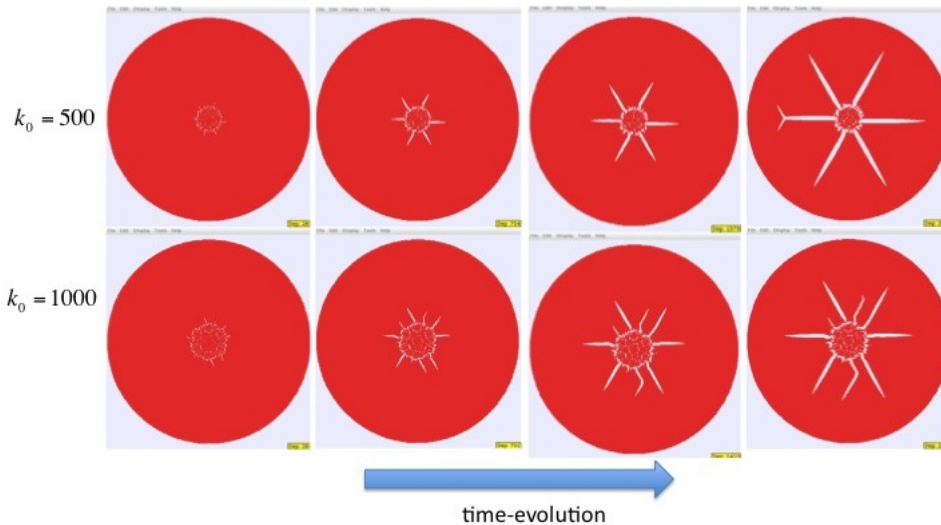


Figure 5. Typical crack evolution patterns for two different impact intensities, quantified by the value of  $k_0$ . The other parameters of the simulations are:  $S = 600 \times 600$ ,  $\eta = 100$ ,  $\rho = 0.85$ ,  $k = 0.4$ ,  $F_{fmax} \in [0, 0.3]$ .

Another striking difference between the patterns in Figure 5 and 2 is that the crack lines in our model are much more straight ones than in reality. We suspect that the reason for this is that the amount of disorder chosen in

the simulation from Figure 5 is not enough. Simulations performed with increased randomness (governed by the interval in which the  $F_{fmax}$  forces are distributed) leads to wiggling crack lines (Figure 6). We conclude thus that in order to get more realistic radially spreading crack lines a higher disorder level should be used. In Figure 6 the unrealistic bifurcation of cracks in the vicinity of the edges is due to the fact that fixed boundary conditions were used, and thus the blocks on the edges are less movable.

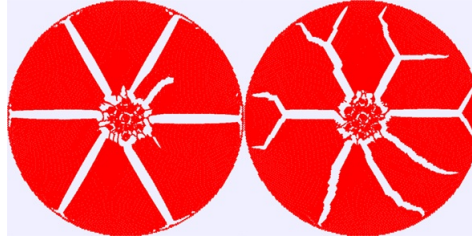


Figure 6. Crack patterns obtained for two different disorder levels in the  $F_{fmax}$  friction force values. The pattern presented in the figure from left is for  $F_f \in [0, 0.2]$  and the pattern presented in the figure from the right is for  $F_{fmax} \in [0, 0.5]$ . The other simulation parameters are:  $S = 400 \times 400$ ,  $\eta = 100$ ,  $\rho = 0.85$ ,  $k = 0.4$ .

Finally, we have performed several simulations in order to study the scaling of the number of radially spreading crack lines as a function of the impact strength, quantified by the value of  $k_0$ . Simulations on systems with sizes  $S = 400 \times 400$  were done, with  $\eta = 100$ ,  $\rho = 0.85$ ,  $k = 0.4$  and  $F_{fmax} \in [0, 0.5]$ . The simulation results are plotted on Figure 7. Although the number of radial cracks were not strictly monotonically increasing with the applied shock intensity, a linear approximation seems acceptable for fitting the obtained data.

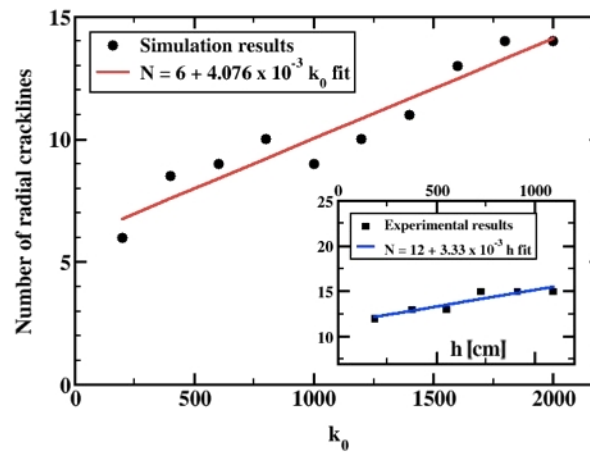


Figure 7. Simulation and experimental results for the scaling of the number of radial cracks as a function of the applied shock. The smaller inset figure presents the experimental results obtained in [42]. The dropping height in the figure is given in  $cm$ . The parameters for the computer simulations are:  $S = 400 \times 400$ ,  $\eta = 100$ ,  $\rho = 0.85$ ,  $k = 0.4$  and  $F_{fmax} \in [0, 0.5]$

## 6. Experiments

The experiments were performed as part of a student project at the National Technical University of Grenoble (France) [42]. The aim of these experiments were to study qualitatively the morphology of the fracture patterns induced by a controlled perpendicular impact on glass plates. The experiments were designed as simple "kitchen experiments", without the claim of a thorough and rigorous experimental investigation. The obtained results are thus only of qualitative nature. The experimental setup was very simple. Glass plates with sizes of  $40\text{cm} \times 40\text{cm}$  and thickness of 4mm were covered from the bottom with a plastic sticker to prevent the spreading of glass after the impact. Preliminary experiments have shown that by changing the thickness of the glass plates one can influence the number of nucleated crack-lines, since a part of the impact energy is used for the in-depth penetration of cracks. Within this student project the thickness dependence was not thoroughly investigated and we have used cheap commercial glass-plates with the same 4mm thickness.

The glass plates were fixed on a surface and a standard petanque ball (with mass of 0.73kg and diameter of 0.075m) was dropped on them from different heights, guided by a plastic tube with adjustable length ( $h \in [2, 10]m$ ). The contact area (crushed region of the glass plate) was disc-shaped with a radius of about 2cm. The experiments were performed in the staircase of the laboratory, and we have to admit the students had a big fun doing them. For each height we have performed only one experiment due to the very limited budget of the project. The experiments were designed for a qualitative mapping, nevertheless ulteriorly we realized that the results could be useful for predicting or confirming simple trends, like the scaling of the number of radially propagating crack lines with the dissipated energy. The lack of repeated experiments for the same height diminishes however the trust in the quantitative data, since there is practically no way to add error-bars. This setup is sketched in Figure 8.

After impact the obtained fracture patterns were recorded and analyzed in different aspects. One aim of the experiments was to elucidate how the number of radial crack lines are varying with the strength of the impact. It is a well-known fact that the growth of a crack requires the creation of two new surfaces and hence an increase in the surface energy. This energy comes from the impact, or in other words one can affirm that during crack propagation the impact energy is dissipated in the newly created surfaces. In the experimental setup the amount of energy dissipated in the impact is directly proportional with the height of the petanque ball's drop. Our modeling assumption is that in the spring-block approach this energy should be transferred in the elastic energy of the springs which in turn is directly proportional with the values fixed for the spring-constants. In such view one might expect that the height of the drop will be equivalent with the the extra  $k_0$  value used in the spring-block model.

Plotting the experimentally obtained radial crack lines as a function of the drop height, an approximately linear trend is obtained in good agreement with the predictions of the simple spring-block approach (inset graph in Fig. 7). We emphasize here again that due to the fact that no error-bars are given for the data-points, one can only qualitatively judge the obtained trend.

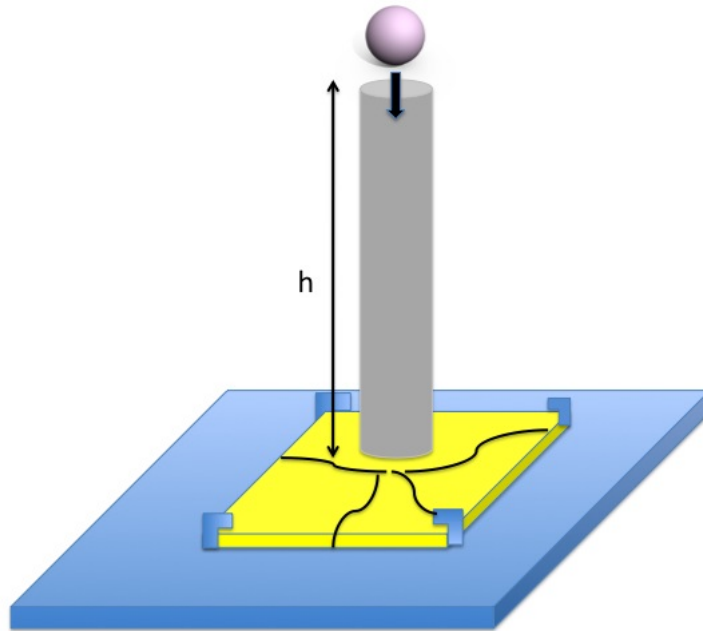


**Figure 8.** Experimental setup.

## 7. Conclusion

A simple spring-block type model was considered for describing the crack patterns obtained in the fracture of glass plates due to a point-like impact. Beside a qualitative reproduction of the experimentally detected radial and circular crack lines, the aim of the study was to get some quantitative results for the scaling of the number of radial crack lines as a function of the strength of the impact. A previously performed student project suggested that the number of radial crack lines varies linearly as a function of the mechanical energy dissipated in the impact.

The specific plasticity and structure of glass was incorporated in the spring-block system by considering an isotropic topology of the spring network and a disorder in the slipping thresholds of the blocks. The energy of the impact was modeled by increasing instantaneously the spring-constant values in the system. The cracks were obtained by relaxing the loaded spring-block system and by breaking all springs that exceeded a threshold tension. Large scale computer simulations were performed for investigating the effect of impact strength and amount of disorder quenched in the model. The computationally generated crack structures were realistic if enough disorder was introduced in the system. In such cases the model reproduced well the experimentally obtained scaling law for the number of radial crack lines as a function of the impact energy.

A secondary aim of the research was to prove once again the usefulness and wide applicability of the simple

spring-block type models. This model family seems especially useful for modeling mesoscopic or macroscopic scale collective phenomena or avalanche like dynamics in complex systems. As the present work exemplifies, it is easily adaptable for various materials and problems, and carries also a pedagogical value since it offers a visual picture on many complex phenomena based on elementary classical mechanics knowledge.

## 8. Acknowledgement

Financial support was provided by the PN2-IDEI-2369/2008 research grant. One of the authors (EÁH) was partly funded by a scholarship from the Heidelberg Graduate School of Mathematical and Computational Methods for the Sciences, University of Heidelberg, Germany, which is funded by the German Excellence Initiative (GSC 220).

## References

- 
- [1] E. Le Bourhis, *Glass: Mechanics and Tehnology* (Wiley-VCH Verlag GmbH @ KGaA, Weinheim, 2008)
  - [2] S.F. Pugh, *Br. J. Appl. Phys.* vol. 18, pp. 129-163 (1967)
  - [3] *Statistical Models for the Fracture of Disordered Media*, edited by H.J. Hermann and S. Roux (North-Holland, Amsterdam, 1990)
  - [4] T. L. Anderson, *Fracture Mechanics: Fundamentals and Applications* (CRC Press, Boca Raton, second edition, 1995)
  - [5] T. Nishioka, *Int. J. Fract.*, vol. 86, 127 (1997)
  - [6] J.A. Astrom, *Advances in Physics*, vol. 55, pp. 247-278 (2006)
  - [7] H.J. Herrmann, F.K. Wittel and F. Kun, *Physica A*, vol. 371, 59 (2006)
  - [8] A. Levandovsky and A.C. Balazs, *Phys. Rev. E* vol. 75, 056105 (2007)
  - [9] J. F. O'Brien and J. K. Hodgins, *Proceedings of the 26th annual conference on Computer graphics and interactive techniques (SIGGRAPH'99)* 137 (1999)
  - [10] J.E. Field, *Contemp. Phys.*, vol. 12, 1 (1971)
  - [11] G. I. Kanel, A. M. Molodets, and A. N. Dremin, *Combust., Explos. Shock Waves* vol. 13, 772 (1977)
  - [12] Z. Rosenberg, D. Yaziv, and S. J. Bless, *J. Appl. Phys.* vol. 58, 3249 (1985)
  - [13] N. S. Brar, S. J. Bless, and Z. Rosenberg, *Appl. Phys. Lett.* vol. 59, 3396 (1991)
  - [14] H. D. Espinosa, Y. Xu, and N. S. Brar, *J. Am. Ceram. Soc.* vol. 80, 2074 (1997)
  - [15] T. Kadono and M. Arakawa, *Phys. Rev. E*, vol. 65, 035107(R) (2002)
  - [16] T. Kadono, M. Arakawa and N. K. Mitani, *Phys. Rev. E*, vol. 72, 045106(R) (2005)
  - [17] J-P. Guin, S.M. Wiederhorn, *Phys. Rev. Lett.* vol. 92, 215502 (2004)
  - [18] A. Momber, *J. Mater. Sci.*, vol. 46, 4494 (2011)
  - [19] D.E. Grady, *Int. J. of Impact Engineering* vol. 38, 446 (2011)

- [20] F. Auerbach F, *Ann. Phys. Chem.* vol. XLIII, 61 (1891)
- [21] T. Ishii and M. Matsushita *J. Phys. Soc. Jap.* vol. 61, 3474 (1992)
- [22] Z. Neda, A. Mocsy and B. Bako, *Mat. Sci. Eng. A*, vol. 169, L1-L4 (1993)
- [23] Y. Brechet and Z. Neda, *Europhys. Lett.*, vol. 32, 475 (1995)
- [24] M. Ausloos, *Solid State Commun.*, vol. 59, 401 (1986)
- [25] M. Ausloos and J.M. Kowalski, *Phys. Rev. B*, vol. 45, 12 830 (1992)
- [26] R. D'hulst, N. Vandewalle and M. Ausloos, *Phys. Rev. E*, vol. 55, 189 (1997)
- [27] T.P. Swiler, J.H. Simmons, A.C. Wright, *J. Non-Crist. Solids*, vol. 182, 68 (1995).
- [28] R. Burridge and L. Knopoff, *Bull. Seism. Soc. Am*, 57, 341-371 (1961)
- [29] B. Gutenberg and C.F. Richter, *Ann. Geofis.*, vol. 9, 1-23 (1956)
- [30] Z. Olami, J.S. Feder J.S. and K. Christensen, *Phys. Rev. Lett.*, vol. 68, 1244-1247 (1992)
- [31] M.A. Lebyodkin, Y. Brechet, Y. Estrin and L.P. Kubin, *Phys. Rev. Lett.* vol. 74, 4758 (1995).
- [32] K. Kovacs, Y. Brechet and Z. Neda *Mod. Sim. Mat. Sci. Eng.* , vol. 13, 1341 (2005)
- [33] F. Jarai-Szabo, B. Sandor and Z. Neda, *Centr. Eur. J. Phys.*, vol. 9, 1002 (2011)
- [34] F. Jarai-Szabo, S. Astilean and Z. Neda, *Chem. Phys. Lett.*, vol. 408, 241 (2005)
- [35] F. Jarai-Szabo, E-A Horvat, R. Vajtai and Z. Neda, *Chem. Phys. Lett.*, vol. 511, 378 (2011)
- [36] J.V. Andersen, Y. Brechet and H.J. Jensen, *Europhys. Lett.*, vol. 26 , 13 (1994)
- [37] K.T. Leung and Z. Neda, *Phys. Rev. Lett.*, vol. 85, 662 (2000)
- [38] K.T. Leung and Z. Neda, *Phys. Rev. E*, vol. 82, 046118 (2010)
- [39] K.T. Leung, L. Jozsa, M. Ravasz and Z. Neda, *Nature*, vol. 410, 166 (2001)
- [40] Z. Neda, K.T. Leung, J. Jozsa and M. Ravasz, *Phys. Rev. Lett.*, vol. 88, 095502 (2002)
- [41] W. A. Curtin and H. Scher, *J. Mater. Res.*, vol. 5, 535 (1990)
- [42] Y. Brechet et. al, private communication, student research project